FY2012

Final Technical Report

Effective Detection of Low-luminosity GEO Objects Using Population and Motion Predictions (AOARD-104136)

Yukihito Kitazawa *

*IHI Corporation, Toyosu IHI Building 1-1, Toyosu 3-chome, Koto-ku, Tokyo, 135-8710 Japan

Report Documentation Page

Form Approved
OMB No. 0704-0188

1. REPORT DATE	2. REPORT TYPE	3. DATES COVERED
03 SEP 2013	**Final**	**09-09-2010 to 06-06-2013**

4. TITLE AND SUBTITLE
Effective Detection of Low-luminosity GEO Objects Using Population and Motion Predictions

5a. CONTRACT NUMBER
FA23861014136

5b. GRANT NUMBER

5c. PROGRAM ELEMENT NUMBER

6. AUTHOR(S)
Yukihito Kitazawa

5d. PROJECT NUMBER

5e. TASK NUMBER

5f. WORK UNIT NUMBER

7. PERFORMING ORGANIZATION NAME(S) AND ADDRESS(ES)
IHI Corporation,1-1, Toyosu 3-chome, Koto-ku,Tokyo,japan,JP,100

8. PERFORMING ORGANIZATION REPORT NUMBER
N/A

9. SPONSORING/MONITORING AGENCY NAME(S) AND ADDRESS(ES)
AOARD, UNIT 45002, APO, AP, 96338-5002

10. SPONSOR/MONITOR'S ACRONYM(S)
AOARD

11. SPONSOR/MONITOR'S REPORT NUMBER(S)
AOARD-104136

12. DISTRIBUTION/AVAILABILITY STATEMENT
Approved for public release; distribution unlimited

13. SUPPLEMENTARY NOTES

14. ABSTRACT

This study applies the orbital debris modeling techniques to devise an effective search strategy applicable for breakup fragments in the geostationary region. The orbital debris modeling describes debris generation and orbit propagation, so that we can effectively conduct predictive analyses of space objects that include characterizing, tracking and predicting the behavior of individual and groups of space objects. Therefore, the techniques enable us to predict population of debris originated from a specific breakup to effectively specify when, where and how we should conduct search surveys using ground-based telescopes. The techniques also enables us to predict two-dimensional motion of debris in successive images taken. The motion prediction can effectively and precisely specify how we should process successive images of objects to be detected. The motion prediction also can clearly distinguish between fragments originated from the target breakup and others. Therefore, the effectiveness of the proposed search strategy is superior to the existing all-sky survey not only in terms of the detection rate but also in terms of the efficiency on origin identification. This report demonstrates characterization of the known US Titan IIIC Transtage explosion in February 1992 using NASA standard breakup model, and the applicability of proposed strategy to a breakup event, which may be uncertain in time within several weeks.

15. SUBJECT TERMS
Space Debris, Space Environment, Situational Awareness, SSA

16. SECURITY CLASSIFICATION OF:			17. LIMITATION OF ABSTRACT	18. NUMBER OF PAGES	19a. NAME OF RESPONSIBLE PERSON
a. REPORT **unclassified**	b. ABSTRACT **unclassified**	c. THIS PAGE **unclassified**	**Same as Report (SAR)**	**18**	

Standard Form 298 (Rev. 8-98)
Prescribed by ANSI Std Z39-18

ABSTRACT

This granted study proposes to apply the orbital debris modeling techniques to devise an effective search strategy applicable for breakup fragments in the geostationary region. The orbital debris modeling describes debris generation and orbit propagation, so that we can effectively conduct predictive analyses of space objects that include characterizing, tracking and predicting the behavior of individual and groups of space objects. Therefore, the techniques enable us to predict population of debris originated from a specific breakup to effectively specify when, where and how we should conduct search surveys using ground-based telescopes. The techniques also enable us to predict two-dimensional motion of debris in successive images taken. The motion prediction can effectively and precisely specify how we should process successive images of objects to be detected. The motion prediction also can clearly distinguish between fragments originated from the target breakup and others. Therefore, the effectiveness of the proposed search strategy is superior to the existing all-sky survey not only in terms of the detection rate but also in terms of the efficiency on origin identification. This report demonstrates characterization of the known US Titan IIIC Transtage explosion in February 1992 using NASA standard breakup model, and the applicability of proposed strategy to a breakup event, which has uncertainty about the time to the order for several weeks.

1. INTRODUCTION

This granted study proposes to apply orbital debris modeling techniques to devise an effective search strategy applicable for breakup fragments in the geostationary region. The orbital debris modeling techniques describe debris generation and orbit propagation to effectively conduct predictive analyses of space objects that include characterizing, tracking and predicting the behavior of individual and groups of space objects. The orbital debris modeling techniques enable us to predict population of debris from a specific breakup to effectively specify when, where and how we should conduct optical measurements using ground-based telescopes. The orbital debris modeling techniques also enable us to predict motion of debris in successive images to effectively and precisely specify how we should process successive images of objects in the geostationary region, taken with ground-based telescopes.

Original (the first year) tried to validate the proposal techniques (population prediction and motion prediction) through actual observations, targeting the US Titan IIIC Transtage (1968-081E) explosion in the geostationary region. As a result, Original successfully demonstrated that population prediction effectively specified when, where, and how we should conduct optical measurements using ground-based telescopes. Original also successfully demonstrated that the motion prediction clearly distinguished fragments generated by the target breakup event from other detected objects that have originated with other breakups. It is concluded from the second demonstration that the motion prediction has a possibility to enhance track-before-detect techniques, which stack successive images shifted according to the assumed motion of the target object.

Option 1 (the second year) confirmed whether or not the combination of the proposal techniques and track-before-detect techniques could detect dimmer objects than the limiting magnitude of a single charged-coupled device (CCD) image taken. Japan Aerospace Exploration Agency (JAXA) has developed the stacking method, a track-before-detect technique. JAXA has applied the stacking method to discover minor planets and successfully discovered many minor planets. JAXA also has applied the stacking method to detect faint objects in the geostationary region but not successfully detected yet. With the proposal techniques, the stacking method successfully detects uncorrelated targets dimmer than the limiting magnitude of a single CCD image. Option 1 also demonstrated the proposal techniques were able to distinguish between multiple events and to identify the right origin by targeting both explosions of the US Titan IIIC Transtage (1968-081E) and the Russian Ekran 2 (1977-092A). With a pinch point analysis, the motion prediction successfully associated uncorrelated targets with the right origin.

According to the outcome of Option 1, Option 2 (the third year) defines three tasks as continuity plan. First, as Task A, Option 2 characterizes the US Titan IIIC Transtage (1968-081E) explosion on 21 February 1992. The NASA standard breakup model 2001 revision [1] describes the size distribution of fragments from an explosion using a simple power-law:

$$N(L) = sf \times 6 \times L^{-1.6} \quad (1)$$

where N is the number of fragments greater than diameter L (in meters), and sf is the scaling factor. Option 2 estimates the scaling factor using the fragments identified through Option 1 based on the proposal techniques. Using the 1968-981E fragments correlated in the catalogue, Option 2 also estimates velocity increment for each fragment to transfer from the orbit of the US Titan IIIC Transtage (1968-081E) at the time of the explosion to their initial orbits after the time of the explosion.

Second, as Task B, Option 2 conducts observation planning based on the outcome of Task A, and then assesses the appropriateness of Task A. Specifically, Task B extracts and analyzes all the differences between the observation plans based on the NASA standard breakup model 2001 revision and the outcome of Task A. Task B conducts another observation when any significant difference can be confirmed.

Finally, as Task C, Option 2 theoretically confirms the applicability of the proposal techniques to a breakup event, which has uncertainty about the time to the order for several weeks. Specifically, Task C selects another US Titan IIIC Transtage (1967-066G), which experienced a significant anomaly in the archived orbital history. Task C predicts the population of possible fragments from 1967-066G with several or more assumptions made on the time, and then tracks all the points where most fragments will be in geocentric equatorial inertial coordinates over time to understand the behavior of groups of the fragments. Task C conducts observations when any significant and effective observation plan can be devised.

2. STRATEGY OVERVIEW

Fig. 1 schematically describes the overview of an effective search strategy that we propose through this granted study. The orbital debris modeling techniques describe debris generation and orbit propagation to effectively conduct predictive analyses of space objects that include characterizing, tracking and predicting the behavior of individual and groups of space objects.

First, fragments from a breakup event in the geostationary region, cited in literature [2–5], are generated using the NASA standard breakup model 2001 revision [1]. Then, their orbits are propagated until the planned observation date to predict population of the generated fragments. There is significant uncertainty in debris generation, so that it is unfeasible or impossible to compute an exact result with a deterministic algorithm. Therefore, a Monte Carlo method has been applied to aggregate the results of the individual computations into the final result. One hundred groups of fragments from a breakup event are computed using a random number generator with 100 different seeds. The mean of 100 computations represents the final result, whereas the standard deviation of 100 computations represents the error of this method.

The resulting population specifies when, where and how optical measurements using ground-based telescopes should be conducted. Second, therefore, "planning and observation" in Fig. 1 is conducted based on the resulting population. A couple of candidate points in geocentric equatorial inertial coordinates can be selected with consideration that bright stars will not be in the field of view. Then, observations are planned to keep looking at

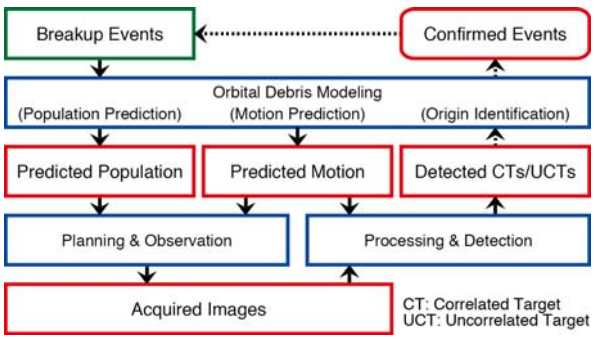

Fig. 1. Approach and workflow.

each point for a relatively long duration. To effectively detect debris in the geostationary region, however, images should be taken with non-sidereal mode. Therefore, one set of images will be taken for several minutes without any tracking, and then the pointing will be changed to keep looking at the specified single point in geocentric equatorial inertial coordinates.

Third, motion of fragments passing through the specified single point in geocentric equatorial inertial coordinates during the observation is predicted based on the resulting population. Motion prediction characterizes the behavior of groups of fragments from a single breakup event. Therefore, the motion prediction can clearly distinguish fragments generated by a target breakup event from other detected objects. The motion prediction also specifies effectively and precisely how successive images should be processed to detect moving objects. Fourth, therefore, the motion prediction is combined with a track-before-detection technique, which stacks successive images shifted according to the assumed motion of the target object, to detect faint fragments from the target breakup event.

Finally, we can analyze how the target breakup event has released fragments based on correlated and uncorrelated targets (CTs/UCTs) detected by the image processing, and then properly describe the target breakup event to improve the debris generation. This improvement provides a better definition of the current situation in the geostationary region.

3. TASK A

Task A characterizes the US Titan IIIC Transtage (1968-081E) explosion on 21 February 1992 using the NASA standard breakup model. The NASA standard breakup model consists of: 1) size distribution to specify the number of fragments for a given size and larger, 2) area-to-mass ratio distribution to specify a possible value for a given size, 3) size-to-area conversion to obtain mass from a given area-to-mass ratio, and 4) delta velocity distribution to specify a possible value for a given area-to-mass ratio.

3.1. Delta Velocity Distribution

Using the 1968-081E fragments correlated in the catalogue, Task A estimates delta velocity for each fragment to transfer to their initial orbits after the time of the explosion from the orbit of 1968-081E at the time of the explosion. Typically, the propagation error is greatest in the along-track direction because time errors greatly displace the satellite along the orbital path. Therefore, instead of applying conjunction analysis, this granted study assumes that fragments were released at the closest position of their initial orbits after the time of the explosion with the orbit of 1968-081E at the time of the explosion.

This granted study estimates delta velocity distribution in a satellite coordinate system, NTW. The T axis is tangential to the orbit and always points to the velocity vector. The N axis lines in the orbital plane and is perpendicular to the velocity vector. The W axis is normal to the orbital plane. Fig.2 shows delta velocity distribution in the NTW system. Symbols "+" represent orthogonal projections of delta velocities on each plane, whereas arrows represent delta velocity of 1968-081E orthographically projected on to each plane. It is obvious that there are major directions of the fragments in each plane and symmetrical features can be confirmed in the major directions. In addition, the delta velocity of 1968-081E points to one of the major directions. As illustrated in Fig. 3, therefore, 1968-081E may have released fragments in two opposite directions. Usually, isotropy is assumed in delta velocities of fragments from a breakup event. Anisotropy may be incorporated to characterize better the US Titan IIIC Transtage explosion, however.

Fig. 4 provides the area-to-mass ratio (A/m) distribution as a function of size (L) and the delta velocity (ΔV) distribution as a function of area-to-mass ratio (A/m). Information on area-to-mass ratio cannot be obtained from a single set of two line elements but we may be able to estimate area-to-mass ratio from archived orbital history. Instead of estimation, however, we assume that the 1968-081E fragments correlated in the catalogue are equal to or larger than 1 m in size (i.e. the nominal limiting size being tracked by the Space Surveillance Network in the geostationary region). With this assumption, a possible range in area-to-mass ratio for the correlated 1968-081E fragments is between 0.027 m^2/kg and 0.584 m^2/kg. With this possible range in area-to-mass ratio, a possible range in the highest delta velocity for the correlated 1968-081E fragments is between 217 m/s and 401 m/s. Fig. 2 indicates that most of the fragments were released at delta velocities lower than 100 m/s. Fig. 2 also indicates that

the highest delta velocity could be up to approximately 200 m/s. Comparison between Figs. 2 and 4 may conclude that 1968-081E may not have released fragments at a relatively high delta velocity, or that 1968-081E may not have released fragments with a relatively high area-to-mass ratio.

3.2. Size Distribution

Using tracklets acquired during the second year, Task A estimates the scaling factor in Eq. (1), which describes the size distribution of fragments from an explosion. The trackles used for this granted study have been acquired through observations from 20 October 2011 to 22 October 2011 at the National Central University (NCU) Lulin Observatory in Taiwan (see also [6]). A 50-cm aperture telescope with a field-of-view of 1.74 degrees by 1.78 degrees at the NCU Lulin Observatory in Taiwan was available for this granted study. As described in Section 2, we conducted observation planning to specify a better point where uncorrelated targets originating from 1968-081E can be detected by using the telescope at the NCU Lulin Observatory in Taiwan.

We were not able to determine precise orbits from the acquired tracklets. We were also not able to conduct backward propagation to identify their right origins, as demonstrated in the previous report. Therefore, we have introduced a probabilistic way to associate the acquired tracklets with 1968-081E. We have applied a k-nearest

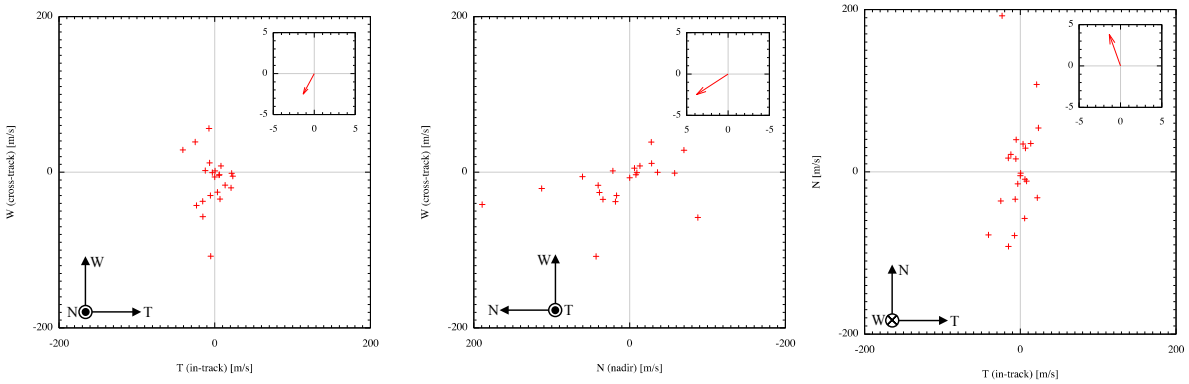

Fig. 2. Delta-velocity distribution of 1968-081E fragments.

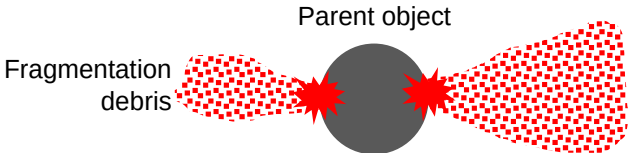

Fig. 3. A possible way for 1968-081E to release fragments.

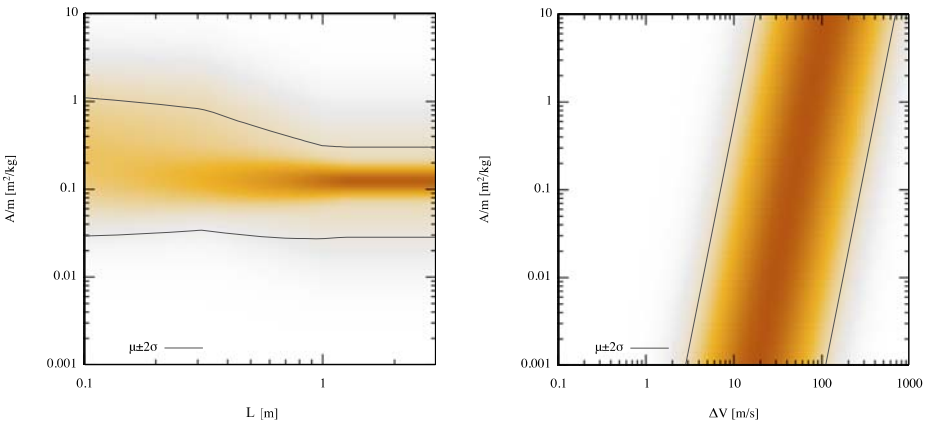

Fig. 4. Area-to-mass ratio and delta-velocity distributions in the NASA standard breakup model 2001 revision.

neighbor method (e.g. [7]) to identify probable origins of the acquired tracklets not correlated with objects in the catalogue. This k-nearest neighbor method requires probable origins to be associated with, so that we refer to [8], which listed 10 events in addition to the known events in the geostationary region, to prepare the probable origins. As presented in [6], 53 tracklets out of 96 tracklets, which were not correlated with objects in the catalogue, has been associated with 1968-081E.

As presented in [9], the characteristic length of each tracklet has been estimated from the brightness. It is assumed that the geometrical configuration is the Lambert sphere with an albedo of 0.1. This assumption defines the characteristic length as the diameter of the Lambert sphere. The size estimation also requires information on ranges and separation angles between the Sun, each object, and the observer, so that a circular orbit is assumed to calculate the initial position at the observation epoch. As also presented in [9], the sensitivity of the optical system at the NCU Lulin Observatory in Taiwan was analyzed to determine the minimum size that can be detected reliably without any fault. Combination of the aforementioned size estimation with this sensitivity analysis may conclude that 31 tracklets out of the 53 tracklets, which were associated with 1968-081E, were detected reliably without any fault.

The aforementioned 31 tracklets may not account for all fragments originating from 1968-081E. Some fragments may not pass through the field-of-view (FOV), so that missing fragments should be incorporated into the size distribution. This granted study has introduced a coefficient R to incorporate the missing fragments into the size distribution. Thus, the right size distribution $N_{event}(L)$ may be given by

$$N_{event}(L) = R \times N_{observation}(L) \tag{2}$$

where $N_{observation}(L)$ represents the size distribution estimated from the 31 tracklets, which were associated with 1968-081E and detected reliably without any fault.

The NASA standard breakup model describes the number of fragments for a given size L and larger as Eq. (1). Among the fragments generated by the NASA standard breakup model, let count only the fragments passing through the FOV. Then, the coefficient R may be defined as

$$R = \frac{N(L)}{N_{FOV}(L)} \tag{3}$$

where $N_{FOV}(L)$ represents the expected number of fragments passing through the FOV for a given size L and larger.

Let consider an orbit with a period of P. If we look at somewhere on the orbit for a given time interval of T, then the coverage of the orbit is calculated by T/P. Using a ground-based optical telescope, we have to consider its FOV, assumed to be fixed somewhere in inertia space. Denoting the time required for an object to ravel in the FOV by Δt, then the coverage of the orbit is $(T + \Delta t)/P$. It may be noted that $\Delta t/P$ provides the effective number, defined as the fractional time, per orbital period, when an object spends in the FOV.

Let assume that K objects, with a given size L and larger, pass through the FOV during the observation. Then, the sum of the coverage of each orbit results in $N_{FOV}(L)$. Thus,

$$N_{FOV}(L) = \sum_{k=1}^{K} \frac{T + \Delta t_k}{P_k} \tag{4}$$

To evaluate the coefficient R in Eq. (3), the scaling factor in Eq. (1) is assumed to be 1.0. The Monte Carlo method described in Section 2 has been also applied to evaluate the coefficient R. The mean of 100 computations represents the nominal value for the coefficient R, whereas the standard deviation of 100 computations represents the error of the coefficient R evaluated. Finally, with the total observation duration summarized in Table 1, Fig. 5 depicts the size distribution of the 1968-081E fragments detected through this granted study. Fig. 5 also plots Eq. (1) with a scaling factor of 2.827 ± 0.013, estimated by applying a least square method.

Table 1. Observation duration at the NCU Lulin Observatory in Taiwan.

Observation date	The number of observations	Observation duration (min)	
		Each	Total
20 Oct. 2011	48	4.6456	222.98
21 Oct. 2011	66	4.2055	277.56
22 Oct. 2011	75	4.2054	315.40

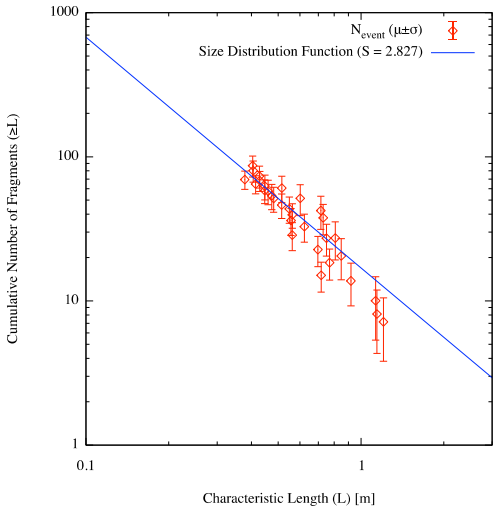

Fig. 5. Size distribution of the 1968-081E fragments detected through this granted study.

A validation of the estimated scaling factor is conducted by calculating the total mass of 10 cm and larger fragments generated by the NASA standard breakup model. The NASA standard breakup model predicts 668 fragments down to 10 cm in size, resulting in a total fragment mass of 1659.7 ± 383.4 kg. As mentioned in [1], the scaling factor of 1.0 appears to be valid for upper stages with masses of 600 – 1000 kg. The mass of 1968-081E after completion of its mission would be approximately 2500 kg, including unused fuel of 500 kg, so that 2.827 ± 0.013 could be a scaling factor in Eq. (1).

4. TASK B

Task B conducts observation planning based on the outcome of Task A, and then assesses the appropriateness of Task A. Specifically, Task B extracts and analyzes all the differences in the observation planning between the NASA standard breakup model and the outcome of Task A.

To extract and analyze all the differences in the observation planning, Fig. 6 compares the time-integrated distributions, which specify where most fragments will be detected, between the initially assumed scaling factor of 1.0 and the estimated scaling factor of 2.827. The duration of the observation is assumed to be 4 hours for this comparison. Deep-colored area represents regions with high detection rates, so that both time-integrated distributions look quite similar. Actually, the observation point specified with the initially assumed scaling factor of 1.0 is identical to that specified with the estimated scaling factor of 2.827. It is concluded, therefore, that observation planning can be conducted properly regardless of the assumed scaling factor.

The detection rates at and around the point are completely different between the two scaling factors, however. This difference may affect the aforementioned probabilistic way of origin identification. Observation planning for fragments not originating from 1968-081E may be also affected by this difference because we may prefer not to specify the point where the 1968-081E fragments will be detected at a higher detection rate.

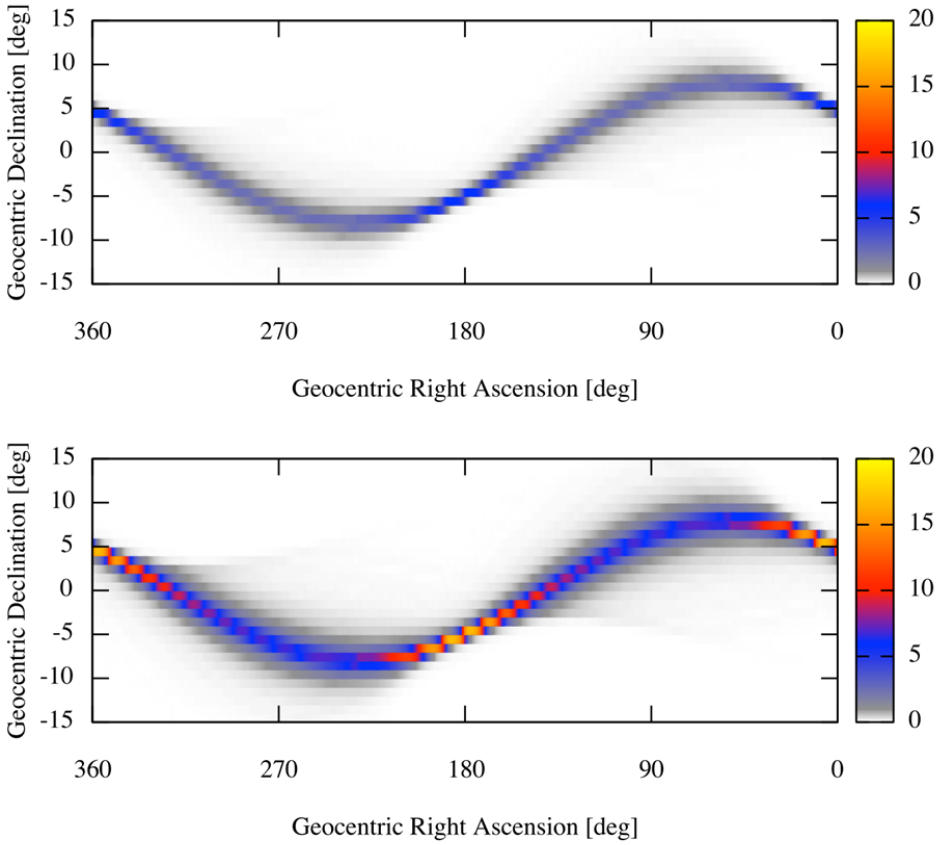

Fig. 6. Comparison in observation planning: (top) with the initially assumed scaling factor of 1.0, and (bottom) with the estimated scaling factor of 2.827.

As mentioned in Subsection 3.1, 1968-081E may have released fragments in two opposite directions. Usually, isotropy is assumed in delta velocities of fragments from a breakup event. Anisotropy may affect the resulting population of the 1968-081E fragments, and so may the observation planning. Therefore, this granted study compares four populations resulted from four different delta velocity distributions in terms of direction such as 1) with an azimuth between 180 and 360 degrees and an elevation between 0 and 90 degrees, 2) with an azimuth of 0 and 180 degrees and an elevation of 0 and 90 degrees, 3) with an azimuth of 0 and 180 degrees and an elevation of –90 and 0 degrees, and 4) with an azimuth of 180 and 360 degrees and an elevation of –90 and 0 degrees. The four populations look slightly different from Fig. 6 but they specify the same point as the observation point. It is concluded, therefore, that observation planning can be conducted properly even assuming isotropy in delta velocities.

5. TASK C

As Fig. 7 reveals, a US Titan IIIC Transtage (1967-066G) has experienced an abrupt orbital change for unknown reasons. As also revealed in [2], no fragments have been yet associated with 1967-066G. On the other hand, 1967-066G has been listed in [8] as those have released fragments to describe the present orbital debris environment in the geostationary region. This abrupt orbital change has uncertainty about the time to the order for several weeks. Therefore, Task C selects 1967-066G to theoretically confirm the applicability of the proposal techniques to such abrupt orbital change, which may have released fragments with uncertainty about the time to the order for several weeks.

5.1. Assumptions

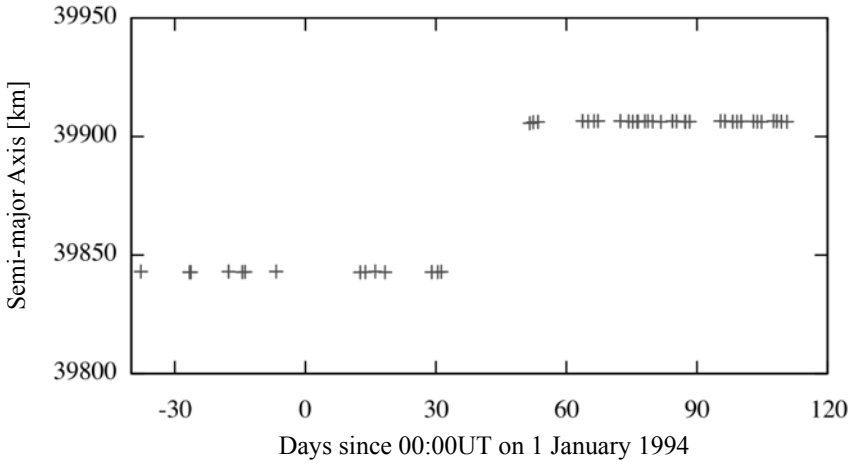

Fig. 7. Abrupt orbital change of 1967-066G for unknown reason

Table 2. Orbital elements of 1967-066G at the start epoch

Epoch	05:09:09 GMT on 1 February 1994
Semi-major axis (km)	39841.866
Eccentricity	0.00535
Inclination (deg.)	11.665
Right ascension of the ascending node (deg.)	25.584
Argument of perigee (deg.)	25.370
Mean anomaly (deg.)	101.179

As Fig. 7 reveals, 1967-066G may have released fragments between 05:09:09 GMT on 1 February 1994 and 14:01:38 GMT on 21 February 1994. This granted study makes 60 assumptions on the date and time of the abrupt orbital change of 1967-066G. The last orbital elements before the abrupt orbital change, given in Table 2, is propagated until the randomly selected date and time of the abrupt orbital change to specify the event location. The NASA standard breakup model is also applied to generate possible fragments from 1967-066G. The scaling factor in Eq. (1) is assumed to be 1.0, resulting in 238 possible fragments down to 10 cm in size from 1967-066G. In total 60 groups of the possible fragments from 1967-066G are computed with 60 different dates and times of the abrupt orbital change. Therefore, this granted study treats the mean of 60 computations as the possible situation.

This granted study applies general perturbation to track all the possible fragments for 54 years, accounting for a period of the geosynchronous precession. This granted study also takes snapshots of the resulting population every 30 days to understand the behavior of groups of the possible fragments. Perturbation forces taken into account for this granted study are the J_2 effect and gravitational attractions due to the Sun and Moon. For simplicity, however, this granted study does not include the J_{22} effect and the solar radiation pressure effects because these effects may not significantly affect their long-term behavior of groups of breakup fragments in the geostationary region. As demonstrated in [10], only 9 fragments out of 238 fragments, with a size of down to 10 cm in size, originating from an explosion at the nominal geostationary altitude might get trapped into the libration region due the J_{22} effect. A preliminary study prior to [10] has also confirmed that the solar radiation pressure effects may not strongly interfere with the long-term behavior of groups of breakup fragments in the geostationary region.

5.2. Long-term Behavior

Fig. 8 demonstrates time variation of the time-averaged distribution of the possible 1967-066G fragments. Fig. 8 also demonstrates time variation of the points with the densest populations of the possible 1967-066G fragments generated on each assumed time of the event. As demonstrated in [11], fragments generated on a specific time of the event form two regions with dense populations at phase positions opposite one another. One of the two regions is at the pinch point where the event has taken place. Right after the time of the event, the regions with dense populations are located along the orbit of 1967-066G, and so do the points with the densest populations. The time-

averaged distribution is drastically changed over time to form two regions with dense populations as fragments generated on a specific time of the event do. This trend can be confirmed from time variation of the points with the densest populations of the possible 1967-066G fragments generated on each assumed time of the event.

Fig. 9 tracks geocentric right ascension and declination of all the points with the densest populations generated on each assumed time of the event. The points with the densest populations converge approximately 3500 days or 9.5

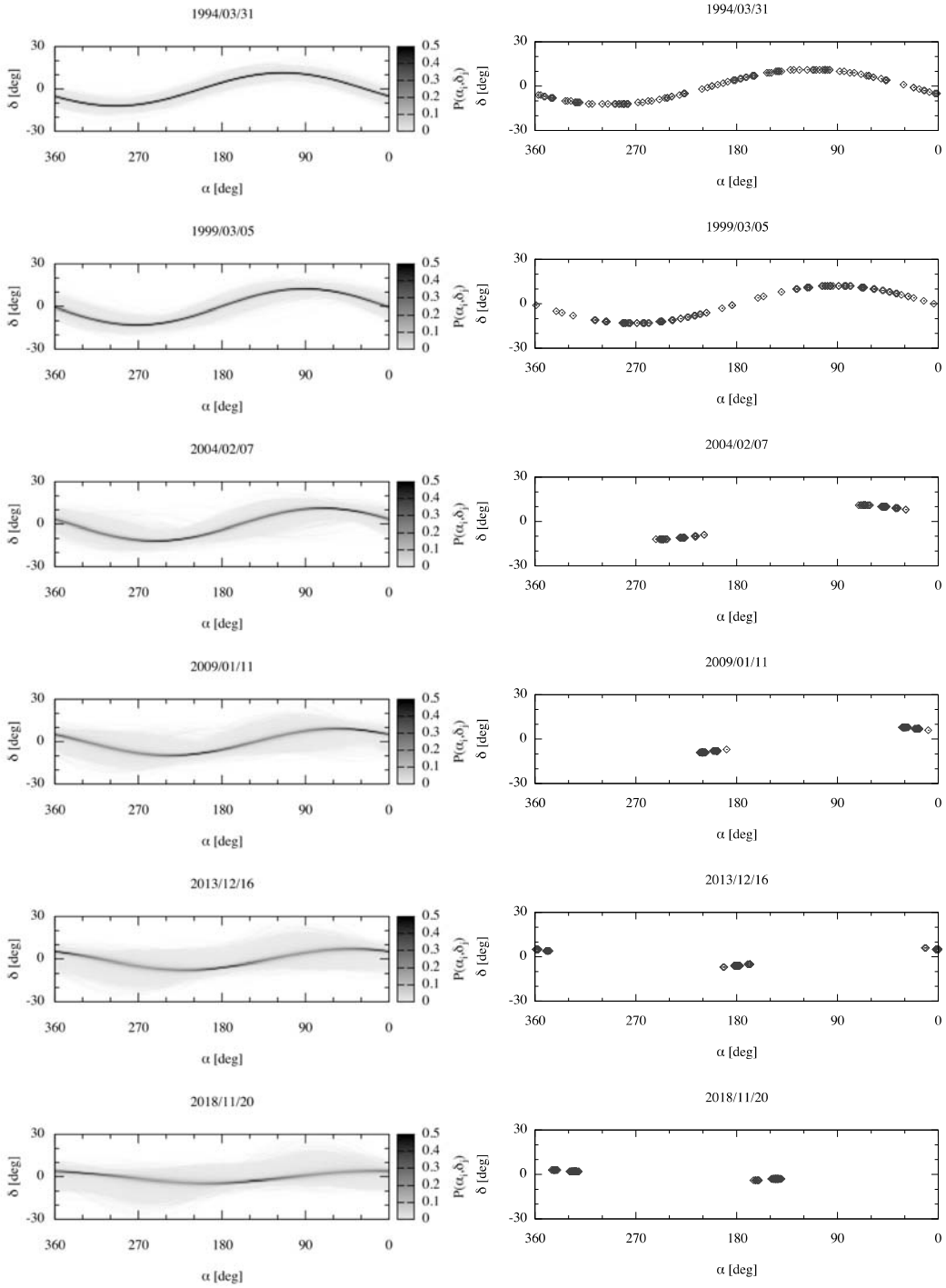

Fig. 8. Population prediction of possible 1967-066G fragments: (left) mean population of 60 assumptions, and (right) the points with the densest populations from each assumption.

years, after the abrupt orbital change. Fig. 9 also demonstrates time variation of the points with the densest populations of the possible 1967-066G fragments generated on each assumed time of the event as in Fig. 8. This time variation may repeat and its period may be consistent with a period of the geosynchronous precession (approximately 54 years). The points with the densest populations spread widely in terms of geocentric right

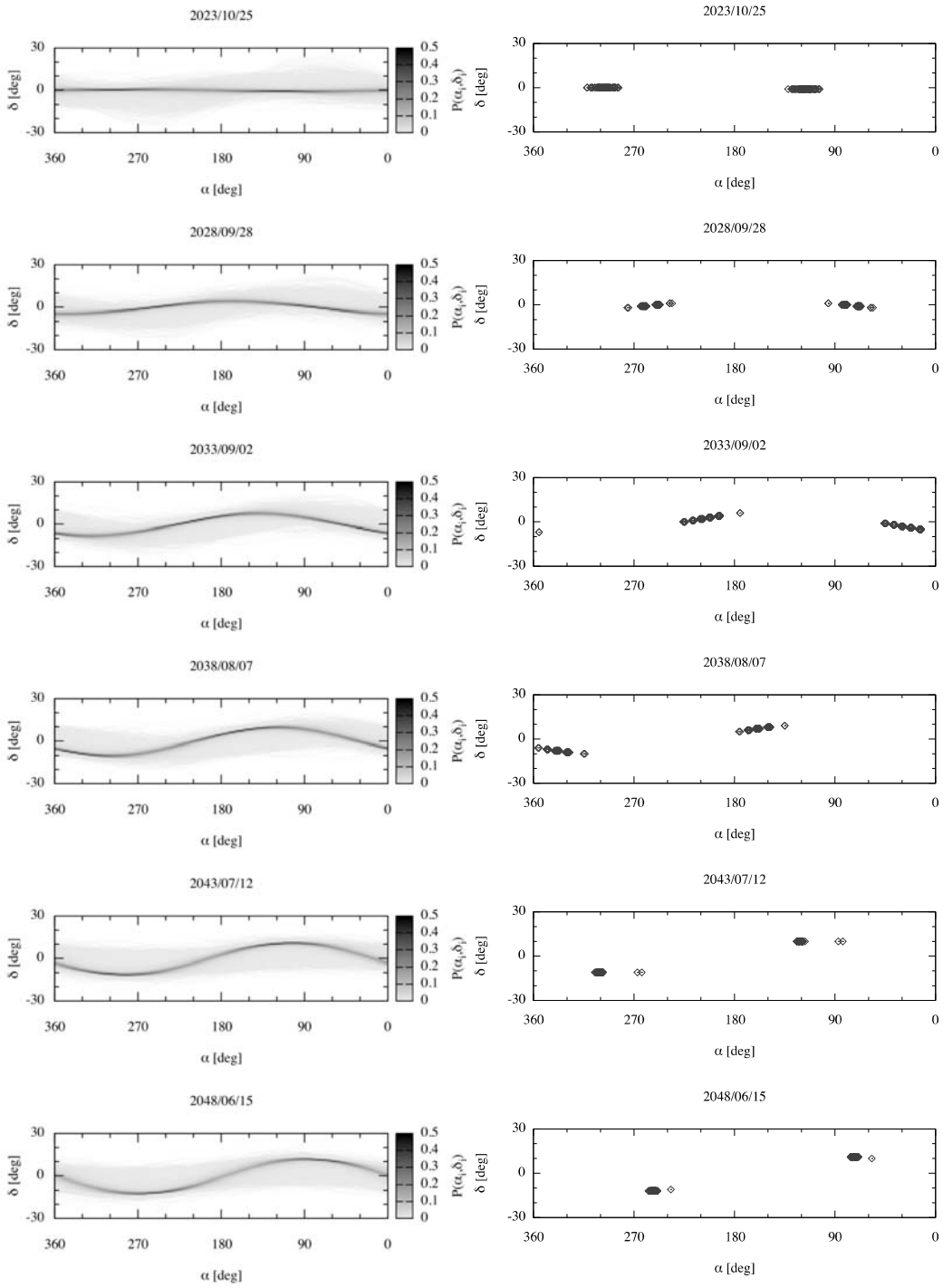

Fig. 8 continued. Population prediction of possible 1967-066G fragments: (left) mean population of 60 assumptions, and (right) the points with the densest populations from each assumption.

ascension around the year 2030 when the inclination of 1967-066G becomes 0 degrees. The points with the densest populations are getting limited in a small region around the year 2045 when the inclination of 1967-066G reaches a heist value. It is concluded, therefore, that any significant and effective observation plan can be devised even with uncertainty about the time of the event to the order for several weeks.

5.3. Observation Planning

JAXA possesses an optical observatory site at Mt. Nyukasa, Nagano Prefecture for research and development on space debris observation technologies and data analysis processes for the geostationary region. The site is at 138º10'18" E, 35º54′05″ N, 1870 m altitude. There are a 35-cm telescope and a 2048 by 2048 CCD camera at the site. The telescope is an $\mathcal{E}$350N manufactured by TAKAHASHI SEISAKUSHO Ltd. Its focal length is 1248 mm. It is set on a fork-type equatorial mount 25 EF manufactured by SHOWA Industry Co., Ltd. The CCD camera is a ML32042, manufactured by Finger Lakes Instrumentation, using a back-illuminated chip, the E2V CCD230-42. The chip is cooled from room temperature down to –60 degrees Celsius with a Peltier device and circulated water. Readout time of the CCD camera is less than 4 seconds. As the pixel size of the chip is 15 μm, the total sky coverage of the image area of the system is around 1.41 degrees by 1.41 degrees, and its pixel scale is 2.2 arc seconds. The start and end time of exposure are recorded in the image header with millisecond accuracy by using a global positioning system (GPS) time recorder which senses the shutter motion.

Observations were planned around the new moon in February 2013 at the JAXA Nyukasa Observatory in Nagano prefecture. Fig. 10 provides the time-averaged distribution of the possible 1967-066G fragments on 10 February 2013 in geocentric equatorial inertial coordinates. Fig. 10 also specifies the visible region from the Observatory and the Earth shadow at the nominal geostationary altitude, both at midnight, for reference. As summarized in Table 3, we select two observation points (Point A and Point B) to maximize observation duration at each night by considering the visible region from the Observatory. We keep looking at Point A for the first half of the night, and then change the pointing of the telescope to keep looking at Point B for the latter half of the night. Observation

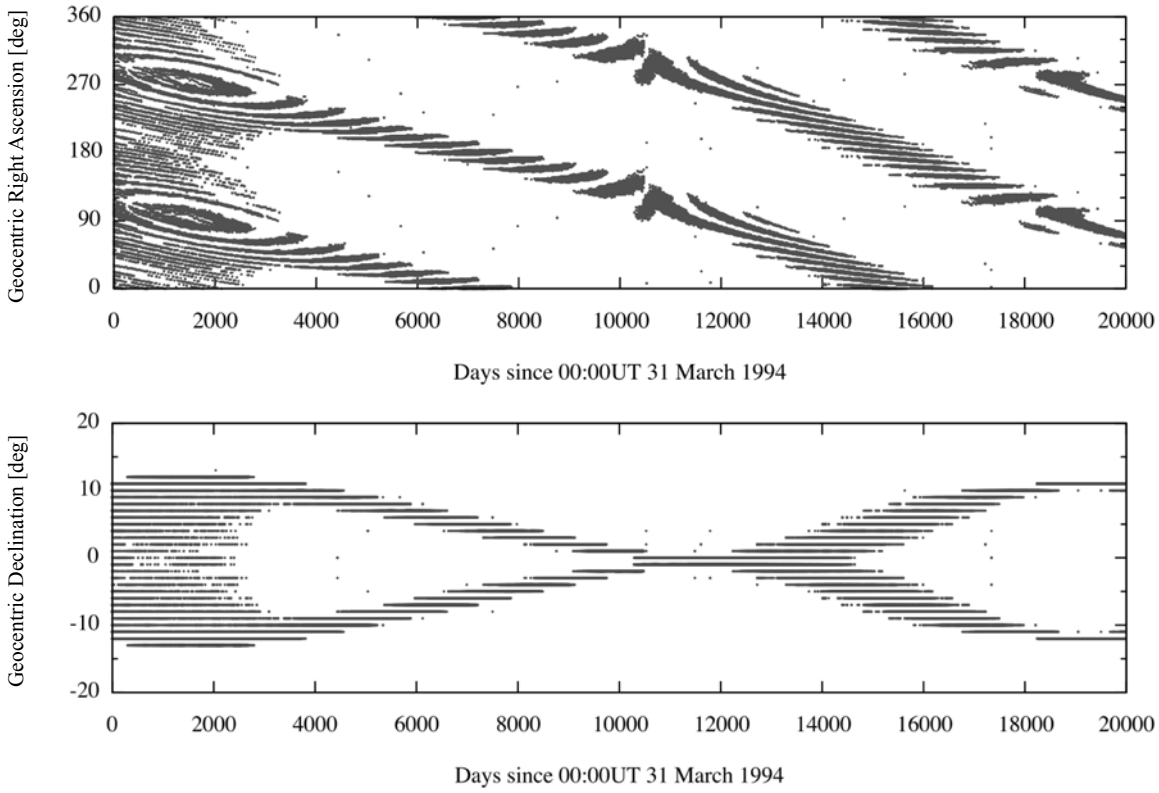

Fig. 9. Time variation of the points with the densest populations of the 1967-066G possible fragments.

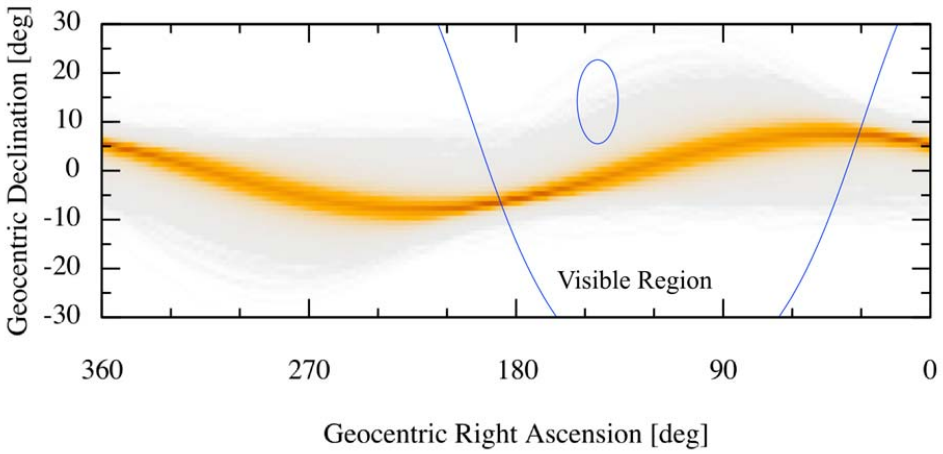

Fig. 10. Observation planning for the possible 1967-066G fragments.

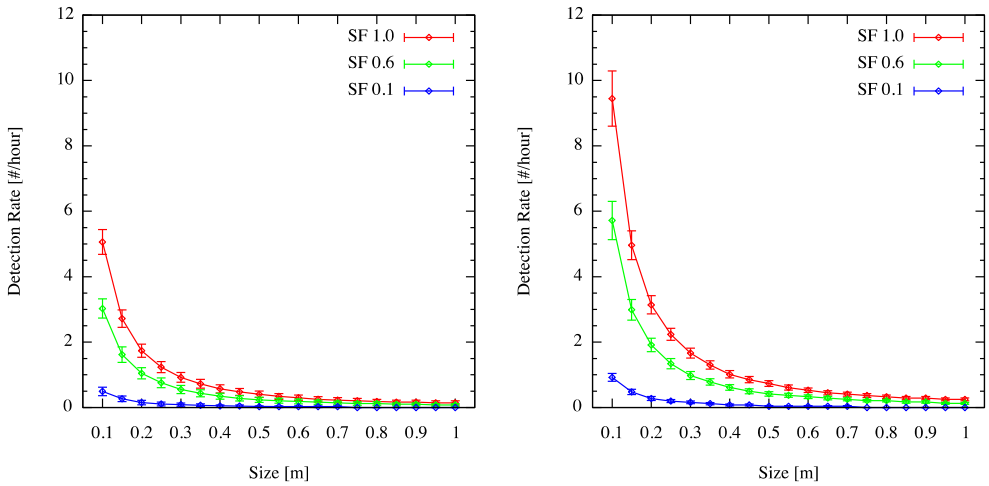

duration night.

The detection rate of the possible 1967-066G fragments at the selected observation points can be evaluated by Eq. (4). Fig. 11 compares the detection rates between the scaling factors of 0.1, 0.6, and 1.0 as a function of the minimum size of the possible 1967-066G fragments. The mean and the standard deviation of the detection rate are evaluated from 100 assumptions on the date and time of the abrupt orbital change of 1967-066G. It can be supposed from Fig. 11 that the Observatory may detect several possible 1967-066G fragments at each observation point if 1967-066G has experienced a major breakup with a scaling factor of 1.0 or great. A US Titan IIIC Transtage of 1968-081E has experienced a major breakup to release relatively large fragments in the catalogue, so that a scaling factor of 1.0 or great may be also possible for 1967-066G. In case of a minor breakup with a scaling factor of 0.1 or so, the Observatory may not be able to detect the possible 1967-066G fragments due to the limit of detection (approximately 30-50 cm).

5.4. Origin Identification

Search surveys of the possible 1967-066G fragments were conducted from 8 February 2013 to 13 February 2013 at the JAXA Nyukasa Observatory in Nagano Prefecture. Fig. 12 compares predicted two-dimensional motion $(\Delta X, \Delta Y)$ of the possible 1967-066G fragments and measured two-dimensional motion of CTs (× in magenta) and UCTs (+ in red) detected at Point A and Point B. Lines in magenta in Fig. 12 represent the "most likely" region, where on average more than one fragments travels in successive images at a given two-dimensional motion, to include approximately 70% of the possible 1967-066G fragments.

Some UCTs appear in the proximity to the boundary of the "most likely" region formed by the possible 1967-066G fragments at Point A. Therefore, these UCTs are unlikely to be associated with 1967-066G. One of the UCTs in the proximity to the boundary of the "most likely" region, labeled JAXA-d0044 (diamond in light green), was successfully followed up to determine its orbit for further investigations. As concluded in Appendix, JAXA-d0044 cannot be associated with 1967-066G. Instead, JAXA-d0044 is quite close to 1968-081J (× in blue), one of the 1968-081E fragments in the catalogue. As also investigated in Appendix, however, JAXA-d0044 cannot be associated with 1968-081E.

The "most likely" region formed by the possible 1967-066G fragments at Point B includes 1967-066A (× in brown) and 1967-066B (× in yellow), both spacecraft released from 1967-066G. This "most likely" approach works well to clearly associate objects inside the "most likely" region with 1967-066G, so that some UCTs inside the "most likely" region may have been released from 1967-066G. We were not able to follow up any UCTs inside the "most likely" region, however. Instead, two UCTs outside the "most likely" region, labeled JAXA-d0045 and -d0046, were successfully followed up to determine their orbits for further investigations. As expected, Appendix concludes that JAXA-d0045 and -d0046 cannot be associated with 1967-066G. Instead, JAXA-d0045 and -d0046 are quite close to CTs launched in the late 70's and early 80's, so that JAXA-d0045 and -d0046 may be associated with these CTs.

6. CONCLUSION

Option 2 (the third year) successfully characterizes the US Titan IIIC Transtage (1968-081E) explosion on 21 February 1992 using the NASA standard breakup model 2001 revision. This characterization concludes that 1968-081E may have released fragments in two opposite directions. However, this granted study confirms that observation planning can be conducted properly even assuming isotropy in delta velocities of the possible 1968-

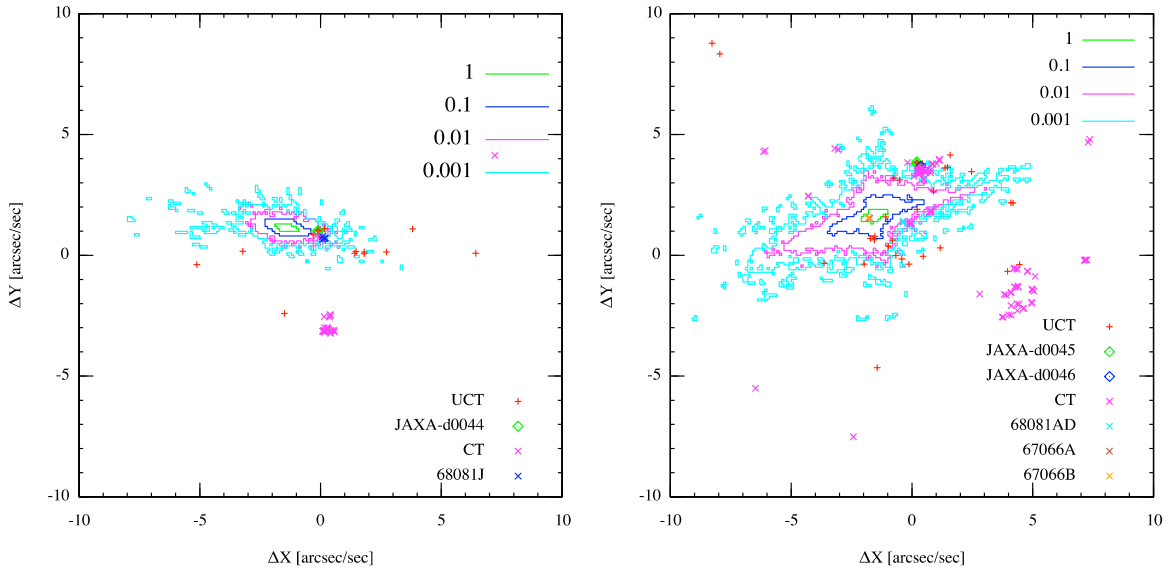

Fig. 12. Comparison in two-dimensional motion between predictions and measurements: (left) Point A, and (right) Point B. Lines in magenta represent the "most likely region" formed by the possible 1967-066G fragments.

081E fragments. This characterization also successfully estimates the scaling factor, which specifies the number of fragments for a given size and larger. It is also confirmed, however, that observation planning can be conducted properly regardless of the assumed scaling factor.

Option 2 theoretically confirms the applicability of proposed strategy to a breakup, which has uncertainty about the time to the order for several weeks. Option 2 also demonstrates observation planning to search possible fragments released from a known orbital anomaly of a US Titan IIIC Transtage (1967-066G) in February 1994. Observations planned for the possible 1967-066G fragments were able to detect some UCTs moving in a field-of-view as predicted. However, we were not able to follow up any of the UCTs moving as predicted to determine their orbits precisely. Therefore, it cannot be concluded that 1967-066G has released the UCTs moving as predicted. Further observations targeting the possible 1967-066G fragments may be required to confirm whether or not 1967-066G has released fragments when 1967-066G experienced the abrupt orbital change.

REFERENCES

1. Johnson, N.L., et al., "NASA's New Breakup Model of Evolve 4.0," *Adv. Space Res.*, Vol.28, No.9, 2001, pp.1377-1384.
2. Johnson, N.L., "Evidence for Historical Satellite Fragmentations in and Near the Geosynchronous Regime," *Proceedings of the Third European Conference on Space Debris, SP-473, Darmstadt, Germany, 2001*, pp.355-359.
3. Rykhlova, L.V., et al., "Explosions on the Geostationary Orbit," *Adv. Space Res., Vol.19*, Issue 2, 1996, pp.313-319.
4. Kiladze, R.I., et al., "On Investigation of Long-term Orbital Evolution of Geostationary Satellites," *Proceedings of the 12th International Symposium on Space Flight Dynamics*, ESA SP-403, 1997, pp.53-57.
5. Sochilina, A.S., et al., "On the Orbital Evolution of Explosion Fragments," Adv. Space Res., Vol.38, 2004, pp.1198-1202.
6. Uetsuhara, M., Yanagisawa, T., Kinoshita, D., Hanada, T., Kitazawa, Y., "Observation Campaign Dedicated to 1968-081E Fragments Identification," accepted for publication in Journal of Advances in Space Research (2013).
7. Bishop, C.M., "Pattern Recognition and Machine Learning," Springer, New York, 2006, pp.122–127.
8. Oswald, M., "New Contributions to Space Debris Environment Modeling," Shaker Verlag GmbH, Germany, 2008.
9. Yanagisawa, T., Kurosaki, H., Uetsuhara, M., et al., "Detection of Small Sized GEO Debris Using FPGA Based Stacking Method," PEDAS.1-0001-12 presented at the 39th COSPAR Scientific Assembly, Mysore, India, July 14-22, 2012.
10. Hanada, T., Yasaka, T., "Orbital Evolution of Cloud Particles from Explosions of Geosynchronous Objects," Journal of Spacecraft and Rockets, Vol.42, No.6, 2005, pp.1070-1076.
11. Uetsuhara, M., Hanada, T., Yamaoka, H., Yanagisawa, T., Kurosaki, H., Kitazawa, Y., "Strategy to Search Fragments from Breakups in GEO," *Adv. Space Res.*, Vol.49, No.7, 2012, pp.1151-1159.

PUBLICATIONS

Journal Papers

1. Hanada, T., Ariyoshi, Y., Uetsuhara, M., Tagawa, M., Chen, H., Tsutsumi, Y., Doi, A., Kawamoto, S., Yanagisawa, T., Hashimoto, K., Kawabe, A., and Kitazawa, Y., "Orbital Debris Modeling and Applications at Kyushu University," *Journal of Space Technology and Science*, Vol.26, No.2, pp.28-47, 2012.
2. Hanada, T., Uetsuhara, M., Yanagisawa, T., Kitazawa, Y., "Effective Search Strategy Applicable for Breakup Fragments in the Geostationary Region," accepted for publication in *Journal of Spacecraft and Rockets*.
3. Uetsuhara, M., Yanagisawa, T., Kinoshita, D., Hanada, T., Kitazawa, Y., "Observation Campaign Dedicated to 1968-081E Fragments Identification," accepted for publication in *Journal of Advances in Space Research*.
4. Uetsuhara, M., Hanada, T., "Practical Method to Identify Orbital Anomaly as Spacecraft Breakup in the Geostationary Region," accepted for publication in *Journal of Advances in Space Research*.

5. Yanagisawa, T., Kurosaki, H., Uetsuhara, M., Kinoshita, D., Hanada, T., Kitazawa, Y., "Detection of Small Sized GEO Debris Using FPGA Based Stacking Method," to be submitted to *Journal of Advances in Space Research*.

Conference Proceedings

1. Uetsuhara, M., Yanagisawa, T., Kinoshita, D., Hanada, T., Kitazawa, Y., "Collaborative Observations to Search 1968-081E Fragments," presented at the Thirty-ninth COSPAR Scientific Assembly, Mysore, India, July 14-22, 2012.
2. Nakaniwa, Y., Uetsuhara, M., Hanada, T., "Practical Method to Identify Orbital Anomaly as Spacecraft Breakup in the Geostationary Region," presented at the Thirty-ninth COSPAR Scientific Assembly, Mysore, India, July 14-22, 2012.
3. Yanagisawa, T., Kurosaki, H., Uetsuhara, M., Kinoshita, D., Hanada, T., Kitazawa, Y., "Detection of Small Sized GEO Debris Using FPGA Based Stacking Method," presented at the Thirty-ninth COSPAR Scientific Assembly, Mysore, India, July 14-22, 2012.
4. Yanagisawa, T., Kurosaki, H., Banno, H., Kitazawa, Y., Uetsuhara, M., Hanada, T., "Comparison Between Four Detection Algorithms for GEO Objects," presented at the 13th Annual Advanced Maui Optical and Spcae Surveillance Technologies Conference, Maui, HI, September 11-14, 2012.
5. Hanada, T., Kitazawa, Y., Yanagisawa, T., Matsumoto, H., "Research and Development on Space Debris Observations and Measurements," presented at the Nineteenth Session of the Asia-Pacific Regional Space Agency Forum (APRSAF-19), Kuala Lumpur, Malaysia, December 11-14, 2012.
6. Hanada, T., Kitazawa, Y., Yanagisawa, T., Matsumoto, H., "Research Topics for Asia-Pacific Regional Collaboration in the Area of Orbital Debris Issues," presented at Workshop on the Protection of Space Environment, sponsored by Ministry of Foreign Affairs of Japan, in Kuala Lumpur, Malaysia, Kuala Lumpur, Malaysia, December 12, 2012.
7. Uetsuhara, M., Hanada, T., Yanagisawa, T., Kitazawa, Y., "Spacecraft Explosion Event Characterization Using Correlated Observations," presented at the 23rd AAS/AIAA Space Flight mechanics Meeting, Kauai, Hawaii, February 10-14, 2013.
8. Uetsuhara, M., Hanada, T., Kitazawa, Y., Yanagisawa, T., "A Search for Possible Breakup Fragments in the Geostationary Region," presented at the Sixth European Conference on Space Debris, Darmstadt, Germany, April 22-25, 2013.
9. Hanada, T., "Orbital Debris Modeling and Applications at Kyushu University," presented at the Seventh Asia-Pacific Conference on Aerospace Technology and Science, Taiwan, May 23-26, 2013.
10. Hanada, T., "Orbital Debris Modeling and Applications at Kyushu University," presented at the Twenty-ninth International Symposium on Space Technology and Science, Nagoya-Aichi, Japan, June 2-9, 2013.
11. Uetsuhara, M., Hanada, T., "An Iterative Search Strategy for Characterizing Spacecraft Breakup Events," presented at the Twenty-ninth International Symposium on Space Technology and Science, Nagoya-Aichi, Japan, June 2-9, 2013.

APPENDIX A

As mentioned in Subsection 5.4, search surveys of the possible 1967-066G fragments were conducted from 8 February 2013 to 13 February 2013 at the JAXA Nyukasa Observatory in Nagano Prefecture. Three UCTs, labeled JAXA-d0044, -d0045, and -d0046, respectively, were successfully followed up to determine their orbits precisely. As Fig. 12 reveals, JAXA-d0044 is in the proximity to the boundary of the "most likely" region formed by the possible 1967-066G fragments at Point A. JAXA-d0045 and -d0046 are outside the "most likely" region formed by the possible 1967-066G fragments at Point B. Therefore, these UCTs are unlikely to be associated with 1967-066G.

First, as summarized in Table A.1, the characteristic length of the three uncorrelated tracklets detected during the search surveys has been estimated from their visual magnitude (labeled V mag). As described in Subsection 3.2, the characteristic length is defined as the diameter of the Lambert sphere with an albedo of 0.1. As summarized in Table A.1, JAXA-d0044 is relatively large. Instead, JAXA-d0045 and -d0046 are relatively small.

Second, orbits of JAXA-d0044, -d0045, and -d0046 are propagated backward until 05:09:09 GMT on 1 February 1994, consistent with epoch of the last orbital elements before the abrupt orbital change (see Table 2). This granted study applies special perturbation, including also the J_{22} effect and the solar radiation pressure effects, not as in Subsection 5.2. An area-to-mass ratio is assumed to be 0.01 m^2/kg for this backward propagation. Table A.2 provides the orbital elements of JAXA-d0044, -d0045, and -d0046 propagated backward until 05:09:09 GMT on 1 February 1994.

As previously reported, this granted study has proposed the use of inclination vectors $(i\cos\Omega, i\sin\Omega)$ to identify the right origins of UCTs. Fig. A.1 plots inclination vectors of JAXA-d0044, -d0045, and -d0046, and 1967-066G at 05:09:09 GMT on 1 February 1994. For reference, Fig. A.1 also plots inclination vectors of 1968-081E and its fragments at 05:09:09 GMT on 1 February 1994. As also reported previously, the initial distribution of breakup fragments forms a straight line, centering on its origin. It can be observed from Fig. A.1 that the 1968-081E fragments (+ in cyan) still keep almost a straight line approximately two years after being released. It can be also

Table A.1. Visual magnitude and size of the three uncorrelated tracklets.

JAXA-d00_	Point	Date and time	V mag	Size (m)
44	A	2013/02/08 13:16:26	14.34	3.03
44	A	2013/02/13 13:14:27	14.35	3.16
45	B	2013/02/09 17:58:25	17.26	0.53
45	B	2013/02/13 17:22:26	16.63	0.70
46	B	2013/02/09 17:38:26	16.60	0.73
46	B	2013/02/13 16:30:26	16.64	0.72

Table A.2. Orbits of JAXA-d0044, -d0045, and –d0046, propagated backward until the time of the abrupt orbital change of 1967-066G.

Orbital elements	JAXA-d0044	JAXA-d0045	JAXA-d0046
Semi-major axis (km)	42131.233	42068.045	41902.138
Eccentricity	0.008	0.020	0.005
Inclination (deg.)	14.246	11.611	11.690
Node (deg.)	15.044	38.139	43.532
Argument of perigee (deg.)	174.940	72.782	158.066

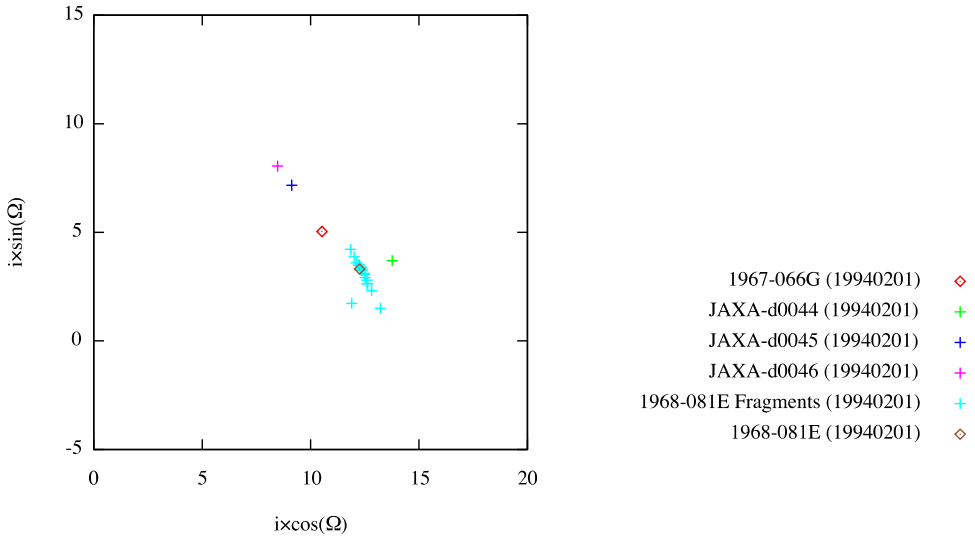

Fig. A.1. Inclination vectors $(i\cos\Omega, i\sin\Omega)$ of UCTs (labeled JAXA-d0044, -d0045, and –d0046, respectively), 1967-066G, 1968-081E, and 1968-081E fragments at the time of the abrupt orbital change of 1967-066G.

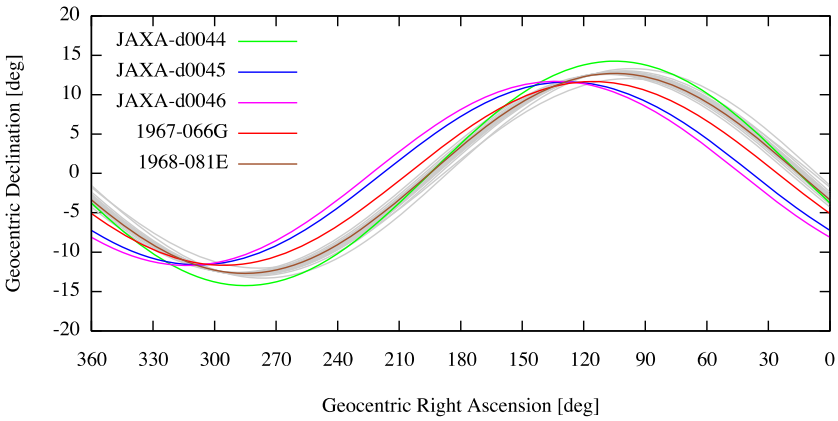

Fig. A.2. Pinch point analysis of UCTs (labeled JAXA-d0044, -d0045, and -d0046, respectively), 1967-066G, and 1968-081E at the time of the abrupt orbital change of 1967-066G.

observed that JAXA-d0045 (+ in blue) and -d0046 (+ in magenta), and 1967-066G lie on a straight line, slightly different from the straight line formed by 1968-081E and its fragments. Therefore, JAXA-d0045 and -d0046 may be associated with 1967-066G, but not with 1968-081E. However, JAXA-d0044 still has the chance to be associated with 1967-066G if JAXA-d0045 and -d0046 may not be associated with 1967-066G.

Third, a pinch point analysis in geocentric equatorial coordinates is applied to identify the right origins of the three UCTs, labeled JAXA-d0044, -d0045, and -d0046, respectively. As previously reported, this pinch point analysis is effective if the origin identification using inclination vectors does not work properly. Fig. A.2 plots the orbits of JAXA-d0044, -d0045, and -d0046, and 1967-066G at 05:09:09 GMT on 1 February 1994. For reference, Fig. A.2 also plots the orbits of 1968-081E and its fragments at 05:09:09 GMT on 1 February 1994. As also previously reported, orbits of fragments originating from a breakup intersect at the same point where the breakup has taken place. It can be observed from Fig. A.2 that 1968-081E (line in brown) and its fragments (lines in light brown) still intersect at almost the same point approximately two years after being released. It can be also observed that JAXA-d0045 (line in blue) and -d0046 (line in magenta), and 1967-066G (line in red) intersect at the same point, slightly different from the intersection of 1968-081E with its fragments. Therefore, JAXA-d0045 and -d0046 may be associated with 1967-066G, but not with 1968-081E. However, JAXA-d0044 still has the chance to be associated with 1967-066G if JAXA-d0045 and -d0046 may not be associated with 1967-066G.

Finally, as in Subsection 3.1, the closest positions of JAXA-d0044, -d0045, and -d0046 with 1967-066G are calculated using their orbits at 05:09:09 GMT on 1 February 1994. The resulting closest positions of JAXA-d0044, -d0045, and -d0046 with 1967-066G are 1934.7 km, 1455.2 km, and 2046.6 km, respectively. It can be concluded, therefore, that JAXA-d0044, -d0045, and -d0046 cannot be associated with 1967-066G.